On the Role of Conical Intersections of Two Potential Energy Surfaces of the Same Symmetry in Photodissociation. 2. $CH_3SCH_3 \rightarrow CH_3S + CH_3$

M. Riad Manaa[†,⊥] **and David R. Yarkony**[*,‡,§]

Contribution from the U.S. Army Research Laboratory, AMSRL-WT-PC, Aberdeen Proving Ground, Maryland 21005-5066, and Department of Chemistry, The Johns Hopkins University, Baltimore, Maryland 21218

Received June 13, 1994[⊗]

Abstract: Methyl disulfide, CH_3SCH_3 is known to exhibit a strong absorption in the 190-210 nm region leading to photofragmentation to CH_3S and CH_3. The role of conical intersections of two states of the same symmetry in this photodissociation process $CH_3SCH_3(X^1A_1) \rightarrow CH_3SCH_3(1,2^1A'') \rightarrow CH_3(X^2A') + CH_3S(X^2E)$ is considered. Points on a surface of conical intersections of the $1,2^1A''$ states in the vicinity of the Franck-Condon region of the X^1A_1 state, accessible with 190-210 nm photons, are determined using configuration interaction wave functions comprised of over 1.2 million configuration state functions. These conical intersections provide an efficient path for the $2^1A''$ state to photodissociate to ground state fragments.

I. Introduction

Recently there has been considerable interest in the ultraviolet photodissociation of polyatomic systems. This interest is motivated in part by the importance of photochemical processes to the chemistry of the upper atmosphere. At ultraviolet wavelengths an excited electronic state may be produced that can decay only nonadiabatically to the observed ground state fragments. The efficiency of such a process depends on the location and character of the region of close approach of the potential energy surfaces. The facility of the nonadiabatic process increases as the separation of the surfaces decreases with a conical intersection providing for maximum efficiency. In this situation, where a single adiabatic state is excited, nonadiabatic effects will be reflected only in the dynamics of the initially prepared wavepacket. However nonadiabatic interactions can also influence a photodissociation process through their effect on the superposition of electronic states initially prepared. This will be particularly evident when the region of electronic nonadiabaticity occurs in the Franck-Condon region of the absorption, and absorption to one of the electronic states is only allowed vibronically, that is, it is symmetry forbidden electronically.

Dimethylsulfide CH_3SCH_3, the doubly methylated analog of dihydrogen sulfide, is potentially interesting in this regard. This molecule has been the object of recent experimental work owing to its significant role in atmospheric sulfur pollution.[1,2] It shows a strong absorption band in the 190-210 nm wavelength region[3,4] that results in the breaking of the C-S bond. In its ground electronic state dimethyl sulfide has C_{2v} symmetry.[1] It has two low-lying excited electronic states, the 1^1B_1 and 1^1A_2 states, in which an electron from a sulfur lone pair, the $3b_1$ orbital, is excited to a Rydberg-like sulfur 4s orbital, the $9a_1$ orbital, or to a C-S antibonding valence-like orbital, the $6b_2$ orbital, respectively. Only the $X^1A_1 \rightarrow 1^1B_1$ transition is symmetry allowed. However when the molecule breaks C_{2v} symmetry as in the dissociation to the ground state products $CH_3S(X^2E)$ and $CH_3(X^2A_1)$, the 1^1B_1, 1^1A_2 states become the $1,2^1A''$ states—assuming for simplicity that a plane of symmetry is preserved—and intensity borrowing is therefore possible. Thus nonadiabatic effects can significantly influence the superposition of electronic states initially prepared.

Conical, or near conical (avoided), intersections may influence the subsequent dynamics of the initially prepared state in this system. Conical intersections of the 1^1B_1 and 1^1A_2 states are symmetry allowed for C_{2v} geometries. However photofragmentation necessarily considers deviations from C_{2v} symmetry. For such nuclear configurations the conical intersections represent intersections of the $1^1A''$ and $2^1A''$ states, two states of the same symmetry. Thus it is essential to be able to characterize "same symmetry" conical intersections. Further to be relevant the conical intersections (i) must be energetically accessible and (ii) should occur in the vicinity of the Franck-Condon region of the X^1A_1 state.

As a consequence of the noncrossing rule for two states of the same symmetry two internal coordinates must be varied in order to locate a conical intersection.[5] However conical intersections determined with *only* two coordinates varied and the remainder (arbitrarily) fixed may miss important geometrical relaxation effects in the other internal degrees of freedom that would serve to make the conical intersection more energetically accessible. This suggests that a detailed knowledge of the potential energy surfaces in question is required to address the issue of geometric relaxation effects, an unpleasant prospect in the present system with its 21 internal degrees of freedom. However this is, in fact, not the case. Conical intersections can be determined *directly*, that is without prior determination of the potential energy surfaces in question, using a recently developed algorithm[6] for which a predetermined—but arbitrary—number of internal coordinates are held fixed and the remainder are optimized to reduce the energy of the points on the surface of conical intersections.[6] In this way the question

† NRC Research Associate.
‡ Supported by DOE Grant DOE-BES Grant DE-FG02-91ER14189.
⊥ U.S. Army Research Laboratory.
§ The Johns Hopkins University.
⊗ Abstract published in *Advance ACS Abstracts*, November 1, 1994.

(1) Nourbakhsh, S.; Norwood, K.; Yin, H.; Liao, C.; Ng, C. Y. *J. Chem. Phys.* **1991**, *95*, 5014.
(2) Lee, Y. R.; Chiu, C. L.; Lin, S. M. *J. Chem. Phys.* **1994**, *100*, 7376.
(3) Clark, L. B.; Simpson, W. T. *J. Chem. Phys.* **1965**, *43*, 3666.
(4) Lee, J. H.; Timmons, R. B.; Stief, L. J. *J. Chem. Phys.* **1976**, *64*, 300.
(5) Herzberg, G.; Longuet-Higgins, H. C. *Disc. Faraday Soc.* **1963**, *35*, 77.
(6) Manaa, M. R.; Yarkony, D. R. *J. Chem. Phys.* **1993**, *99*, 5251.

0002-7863/94/1516-11444$04.50/0

of geometric relaxation effects can be efficiently addressed in a quantitative manner.

This study considers nonadiabatic effects in the photodissociation of dimethyl sulfide. Photoabsorption, $X^1A_1 \rightarrow 1,2^1A''$, will be considered. It will emerge that for small distortions from C_{2v} symmetry a significant transition moment to the $2^1A''$ state exists. It will then be shown that conical intersections of the $1,2^1A''$ states provide an efficient path for dissociation of the $2^1A''$ state into ground state fragments. This study will complement recent studies of photodissociation of dihydrogen sulfide (H_2S)[7,8] and methyl mercaptan, CH_3SH,[9,10] the singly methylated analog of H_2S. In a recent study of methyl mercaptan[10] it was shown that following direct excitation of the $2^1A''$ state ground state photofragments could be efficiently produced through a surface of conical intersections of the $1^1A''$ and $2^1A''$ potential energy surfaces. The H_2S studies on the other hand have focussed on C_{2v} conical intersections,[11,12] and it will emerge that the present study provides potentially interesting insights in that regard.

Section II discusses our theoretical approach, providing a brief overview of our treatment of conical intersections and a description of the state-averaged multiconfiguration self-consistent field (SA-MCSCF)[13-16]/configuration interaction (CI)[17] wave functions used to describe the states in question. Section III presents the results of our calculations, and section IV summarizes and discusses directions for future investigation.

II. Theoretical Approach

A. Locating Conical Intersections of Two States of the Same Symmetry. A point on the surface of conical intersection of two states of the same symmetry subject to a set of geometric equality constraints of the form $C_i(\mathbf{R}) = 0, i = 1,M$ where $\mathbf{R}$ are the nuclear coordinates is determined[6] from the following Newton-Raphson equations

$$\begin{bmatrix} \mathbf{Q}^{IJ}(\mathbf{R},\xi,\lambda) & \mathbf{g}^{IJ}(\mathbf{R}) & \mathbf{h}^{IJ}(\mathbf{R}) & \mathbf{k}(\mathbf{R}) \\ \mathbf{g}^{IJ}(\mathbf{R})^\dagger & 0 & 0 & \mathbf{0} \\ \mathbf{h}^{IJ}(\mathbf{R})^\dagger & 0 & 0 & \mathbf{0} \\ \mathbf{k}(\mathbf{R})^\dagger & \mathbf{0}^\dagger & \mathbf{0}^\dagger & \mathbf{0} \end{bmatrix} \begin{bmatrix} \delta\mathbf{R} \\ \delta\xi_1 \\ \delta\xi_2 \\ \delta\lambda \end{bmatrix} =$$

$$- \begin{bmatrix} \mathbf{g}^I(\mathbf{R}) + \xi_1\mathbf{g}^{IJ}(\mathbf{R}) + \xi_2\mathbf{h}^{IJ}(\mathbf{R}) + \sum_{i=1}^{M}\lambda_i\mathbf{k}^i(\mathbf{R}) \\ \Delta E_{IJ}(\mathbf{R}) \\ 0 \\ \mathbf{C}(\mathbf{R}) \end{bmatrix} \begin{matrix} \text{(2.1a)} \\ \text{(2.1b)} \\ \text{(2.1c)} \\ \text{(2.1d)} \end{matrix}$$

where ξ and λ are Lagrange multipliers, and $\delta\mathbf{R} = \mathbf{R}' - \mathbf{R}$, $\delta\lambda = \lambda' - \lambda$, $\delta\xi = \xi' - \xi$, $\Delta E_{IJ}(\mathbf{R}) \equiv E_I(\mathbf{R}) - E_J(\mathbf{R})$, $g^I_\alpha(\mathbf{R}) \equiv \partial E_I(\mathbf{R})/\partial R_\alpha$, $g^{IJ}_\alpha(\mathbf{R}) \equiv \partial\Delta E_{IJ}(\mathbf{R})/\partial R_\alpha$, $k^i_\alpha(\mathbf{R}) \equiv \partial C_i(\mathbf{R})/\partial R_\alpha$, $h^{IJ}_\alpha(\mathbf{R}) \equiv \mathbf{c}^{I\dagger}(\mathbf{R})\partial\mathbf{H}^e(\mathbf{R})/\partial R_\alpha\mathbf{c}^J(\mathbf{R})$, and $\mathbf{Q}^{IJ}(\mathbf{R},\xi,\lambda)$ is a matrix of second derivatives.[6] Here $\mathbf{H}^e(\mathbf{R})$ is the electronic Hamiltonian matrix in the nonrelativistic Born-Oppenheimer approximation and the electronic (MCSCF/CI) wave function in the configuration state function (CSF) $[\psi(\mathbf{r};\mathbf{R})]$ basis[17] with energy $E_I(\mathbf{R})$ is given by $\psi_I(\mathbf{r};\mathbf{R}) = \sum_\alpha \mathbf{c}^I_\alpha(\mathbf{R})\psi_\alpha(\mathbf{r};\mathbf{R})$. The excellent performance of this algorithm has been documented previously.[6,10]

Equations 2.1 can be motivated as follows. $\mathbf{R}^c$ is sought so that $E_I(\mathbf{R})$ is minimized subject to the constraints $E_I(\mathbf{R}) = E_J(\mathbf{R})$ and $\mathbf{C}(\mathbf{R}) = \mathbf{0}$. The key is to impose the constraint $E_I(\mathbf{R}) = E_J(\mathbf{R})$ noting that at each step in the Newton-Raphson procedure $\mathbf{c}^I(\mathbf{R})$ and $\mathbf{c}^J(\mathbf{R})$ are eigenvectors. Equations 2.1 are the Newton-Raphson equations corresponding to the Lagrangian function[18]

$$L_{IJ}(\mathbf{R},\xi,\lambda) = E_I(\mathbf{R}) + \xi_1\Delta E_{IJ}(\mathbf{R}) + \xi_2 H_{IJ}(\mathbf{R}) + \sum_{k=1}^{M}\lambda_k C_k(\mathbf{R}) \tag{2.2}$$

provided the gradient of $H_{IJ}(\mathbf{R})$ is interpreted as a change in $\mathbf{H}^e(\mathbf{R})$ within the subspace spanned by $\mathbf{c}^I(\mathbf{R})$ and $\mathbf{c}^J(\mathbf{R})$. This can be understood from two perspectives. Assume for convenience that $M = 0$, that is, there are no geometrical constraints.

Consider $\mathbf{R}$ for which eq 2.1 is not satisfied. The 2×2 matrix $\mathbf{H}(\mathbf{R})$ with matrix elements $\mathbf{H}_{KL}(\mathbf{R})$, K,L $\in$ (*I*,*J*) becomes at $\mathbf{R} + \delta\mathbf{R}$

$$\mathbf{H}_{IJ}(\mathbf{R} + \delta\mathbf{R}) = \mathbf{c}^{I\dagger}(\mathbf{R})\left(\mathbf{H}^e(\mathbf{R}) + \sum_\alpha \frac{\partial\mathbf{H}^e(\mathbf{R})}{\partial R_\alpha}\delta R_\alpha\right)\mathbf{c}^J(\mathbf{R}) \tag{2.3a}$$

$\mathbf{H}(\mathbf{R})$ is diagonal but *nondegenerate* at $\mathbf{R}$ that is

$$\mathbf{H}(\mathbf{R}^c) = \begin{bmatrix} E_I(\mathbf{R}) - E_J(R) & 0 \\ 0 & 0 \end{bmatrix} \tag{2.3b}$$

From eq 2.3a at $\mathbf{R}^c = \mathbf{R} + \delta\mathbf{R}$, $\mathbf{H}(\mathbf{R}^c)$ becomes, to first order

$$\mathbf{H}(\mathbf{R}^c) = \begin{bmatrix} \Delta E_{IJ}(\mathbf{R}) + \mathbf{g}^{IJ\dagger}\cdot\delta\mathbf{R} & \mathbf{h}^{IJ\dagger}\cdot\delta\mathbf{R} \\ \mathbf{h}^{IJ\dagger}\cdot\delta\mathbf{R} & 0 \end{bmatrix} \tag{2.3c}$$

Thus eqs 2.1b,c are seen to be the requirement that $\mathbf{H}(\mathbf{R}^c)$ has degenerate eigenvalues, with eigenvectors $\mathbf{c}^I$ and $\mathbf{c}^J$.

At convergence $\mathbf{H}_{IJ}(\mathbf{R}^c)$ is diagonal and *degenerate*. From eq 2.1a $E_I(\mathbf{R}^c)$ has been minimized, $\mathbf{g}^I(\mathbf{R}^c) = \mathbf{0}$, except along directions contained in the two-dimensional subspace spanned by $\mathbf{g}^{IJ}(\mathbf{R}^c)$ and $\mathbf{h}^{IJ}(\mathbf{R}^c)$. From eq 2.3c it is these two directions that lift the degeneracy of $\mathbf{H}(\mathbf{R}^c)$. It is the minimization of $E_I(\mathbf{R}^c)$ in the orthogonal complement of the subspace spanned by $\mathbf{g}^{IJ}(\mathbf{R}^c)$ and $\mathbf{h}^{IJ}(\mathbf{R}^c)$ that results in the "geometrical relaxation effects" noted in the Introduction. A discussion of these points from an alternative perspective has been presented by Radazos *et al.*[19]

Equation 2.1d has its origins in the constraint $\mathbf{C}(\mathbf{R}) = \mathbf{0}$ and enables the searching procedure to be restricted to particular regions of nuclear coordinate space. In this work $\mathbf{C}(\mathbf{R}) = \mathbf{0}$ will be used to restrict one of the C-S bonds to the Franck-Condon region of the ground state. The remaining bond distances will be unconstrained in order to consider the possibility of geometrical relaxation effects.

A solution to eq 2.1 will be referred to as a conical intersection although rigorously degenerate states cannot be obtained from a numerical procedure. If required, the existence of a conical intersection can be rigorously established by

(7) Weide, K.; Staemmler, V.; Schinke, R. *J. Chem. Phys.* **1990**, *93*, 861.
(8) Schinke, R. *Photodissociation Dynamics, Spectroscopy and Fragmentation of small polyatomic molecules*; Cambridge University Press: Cambridge, 1993.
(9) Jensen, E.; Keller, J. S.; Waschewsky, G. C. G.; Stevens, J. E.; Graham, R. L.; Freed, K. F.; Butler, L. J. *J. Chem. Phys.* **1993**, *98*, 2882.
(10) Yarkony, D. R. *J. Chem. Phys.* **1994**, *100*, 3639.
(11) Theodorakopoulos, G.; Petsakalais, I. D. *Chem. Phys. Lett.* **1991**, *178*, 475.
(12) Heumann, B.; Duren, R.; Schinke, R. *Chem. Phys. Lett.* **1991**, *180*, 583.
(13) Docken, K.; Hinze, J. *J. Chem. Phys.* **1972**, *57*, 4928.
(14) Hinze, J. *J. Chem. Phys.* **1973**, *559*, 6424.
(15) Werner, H.; Meyer, W. *J. Chem. Phys.* **1981**, *74*, 5794.
(16) Lengsfield, B. H. *J. Chem. Phys.* **1982**, *77*, 4073.
(17) Shavitt, I. *The Method of Configuration Interaction*, in *Modern Theoretical Chemistry*; Schaefer, H. F., Ed.; Plenum Press: New York, 1976; p 189.
(18) Fletcher, R. *Practical Methods of Optimization*; John Wiley and Sons: New York, 1981.
(19) Radazos, I. N.; Robb, M. A.; Bernardi, M. A.; Olivucci, M. *Chem. Phys. Lett.* **1992**, *197*, 217-223.

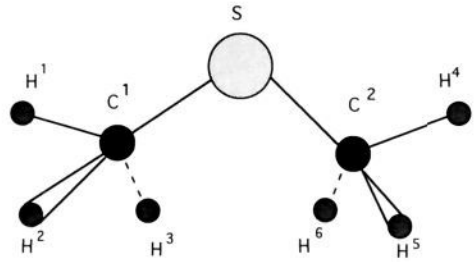

Figure 1. Labeling of atoms in CH_3SCH_3. In C_s symmetry H^2 and H^3 are symmetry equivalent as are H^5 and H^6.

showing that the geometric or Berry phase criterion[5,20] is satisfied, that is the wave function changes sign when a closed path around the point in question is traversed.[21]

B. Electronic Structure Treatment. In this study contracted Gaussian basis sets of (8s6p1d), (4s2p1d), and (2s1p) quality on sulfur, carbon, and hydrogen, respectively, were used. The sulfur basis is that used in the previously noted study of CH_3SH,[10] while the carbon and hydrogen bases are standard double-ζ polarization bases.[22] All calculations were performed in C_s symmetry, see Figure 1. The use of C_s symmetry is a computational convenience, also used in previous theoretical studies of CH_3SH,[9,10] and amounts to the neglect of CH_3 internal rotation, expected to have limited effect on the photodissociation process.

The ground state of dimethyl sulfide corresponds to the C_{2v} electron configuration

$$[1-6a_1^2\ 1-2b_1^2\ 1-4b_2^2\ 1a_2^2]\ \{7-8a_1\ 5b_2\ 3b_1\}^8 \quad (2.4)$$

The orbitals in the square brackets, treated as core orbitals in this work, correspond to the carbon 1s orbitals, the sulfur 1s, 2s, and 2p orbitals, and the CH σ-bonding orbitals. The orbitals in the curly brackets correspond to the CS σ-bonding orbitals and two sulfur lone-pair orbitals. The excited states in question correspond to excitations from the $3b_1$ orbital, the highest occupied molecular orbital,[1] to the sulfur 4s Rydberg orbital or the CS antibonding σ-orbitals, collectively the $9-10a_1$ and $6b_2$ orbitals. Thus in this work an eight electron active space including the $7-10a_1$, $5-6b_2$, and $3b_1$ orbitals, the $11-16a'$ and $4a''$ orbitals in C_s symmetry, was employed. A complete active space[23-25] SA-MCSCF procedure was used to define the molecular orbitals with one $^1A'$ and two $^1A''$ states averaged with weight vector $\mathbf{w} = (1.0, 0.45, 0.55)$. The CI wave functions were expanded in second order CI (SOCI)[26] CSF spaces based on this active space, comprised of 1 281 714 and 1 261 092 CSFs in $^1A'$ and $^1A''$ symmetry, respectively. In these expansions the five a′ and one a″ molecular orbitals with the highest orbital energies were truncated. These large CSF expansions were employed to provide a reliable description of the electronically excited states and represent the largest CSF space used to date to characterize a section of a surface of conical intersection of two states of the same symmetry.

(20) Berry, M. V. *Proc. R. Soc. Lond. Ser. A* **1984**, *392*, 45.
(21) Xantheas, S.; Elbert, S. T.; Ruedenberg, K. *J. Chem. Phys.* **1990**, *93*, 7519.
(22) Dunning, T. H.; Hay, P. J. *Gaussian Basis Sets for Molecular Calculations*, in *Modern Theoretical Chemistry*; Schaefer, H. F., Ed.; Plenum: New York, 1976.
(23) Siegbahn, P.; Heiberg, A.; Roos, B.; Levy, B. *Phys. Scr.* **1980**, *21*, 323.
(24) Roos, B. O.; Taylor, P. R.; Siegbahn, P. E. M. *Chem. Phys.* **1980**, *48*, 157.
(25) Roos, B. O. *Int. J. Quantum Chem. Symp.* **1980**, *14*, 175.
(26) Silverstone, H. J.; Sinanoglu, O. *J. Chem. Phys.* **1966**, *44*, 1899.

Table 1. Points on the Surface of Conical Intersections from SOCI Wave Functions[a]

$R(C^1S)$	$R(C^2S)$ C^1SC^2	$E(1^1A'')$	ΔE	$R(C^1H^1)$ $R(C^1H^2)$	$R(C^2H^4)$ $R(C^2H^5)$	$\angle SC^1H^1$ $\angle SC^2H^4$
3.33	3.735 480	48 954	0.756	2.058 442	2.073 900	109.8
	111.2			2.050 121	2.049 695	105.5
3.43	3.729 084	48 559	0.644	2.064 311	2.067 530	108.5
	111.5			2.053 197	2.041 667	106.6
3.53	3.722 179	48 445	0.770	2.067 079	2.063 382	107.2
	112.0			2.052 281	2.040 096	107.1
3.63	3.700 508	48 504	0.295	2.058 436	2.054 628	105.8
	112.6			2.044 969	2.043 020	107.4

[a] $R(C^1S)$ fixed at indicated value. All other internuclear coordinates optimized using eq 2.1. $R(XX)$ in au, angles in deg. $\Delta E \equiv E(2^1A'') - E(1^1A'')$ in cm^{-1}. $E(1^1A'')$ in cm^{-1} relative to $E(\tilde{X}^1A') = -476.905\ 5576$ au obtained at reference structure $r_e(C^1S) = 3.489$, $r_e(C^2S) = 3.490$, $\angle C^1SC^2 = 105.5$, $r_e(C^1H^1) = 2.051$, $r_e(C^1H^2) = 2.047$, $\angle SC^1H^1 = 104.5$, $\angle SC^1H^2 = 112.4$, $r_e(C^2H^4) = 2.051$, $r_e(C^2H^5) = 2.047$, $\angle SC^2H^4 = 104.5$, $\angle SC^2H^5 = 112.4$, using the labeling in Figure 1.

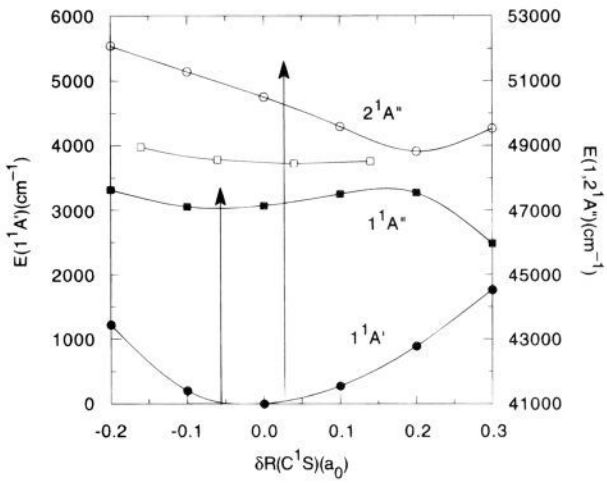

Figure 2. $E(X^1A')$, solid circle, $E(1^1A'')$, solid square, and $E(2^1A'')$, open circle, as function of $\delta R(C^1S)$ with remaining geometrical parameters fixed at the SOCI $\tilde{X}^1A_1$ equilibrium structure indicated in Table 1. $E_x = E(1^1A'') = E(2^1A'')$, open square—conical intersection points for which $\delta R(C^1S)$ is fixed at the indicated value with the remaining geometrical parameters optimized, using eq 2.1 as described in text. All energies in cm^{-1} relative to value at $\tilde{X}^1A_1$ predicted equilibrium structure, $E(\tilde{X}^1A') = -476.905\ 5576$ au, see Table 1. The range of excitation energies (190−210 nm) available for photoexcitation is given by the vertical arrows.

III. Results and Discussions

The qualitative aspects of the photodissociation process are provided in Figures 2 and 3. Figure 2 reports potential energy curves as a function $R(C^1S)$. The remaining internuclear distances are fixed at the equilibrium structure of the X^1A_1 state, denoted $r_e(XY)$, obtained from the SOCI treatment noted in section II. The key geometrical parameters for this structure are given in the footnote to Table 1. In Figures 2 and 3 and the discussion that follows it is convenient to define $\delta R(XY) \equiv R(XY) - r_e(XY)$. It is evident from Figure 2 that the ground state energy is not a strong function of $\delta R(C^1S)$ for $-0.1 < \delta R(C^1S) < 0.1$ so that $r_e(CS)$ is expected to be sensitive to the level of treatment. However a concomitant of this weak $\delta R(C^1S)$ dependence of $E(X^1A_1)$ will be a broad Franck−Condon region of the ground vibrational state so that a precise value for $r_e(CS)$ is not essential in the present treatment. (The slight asymmetry of the X^1A_1 potential energy curve about $\delta R(C^1S) = 0$ reflects the convergence tolerance used in the geometry optimization.)

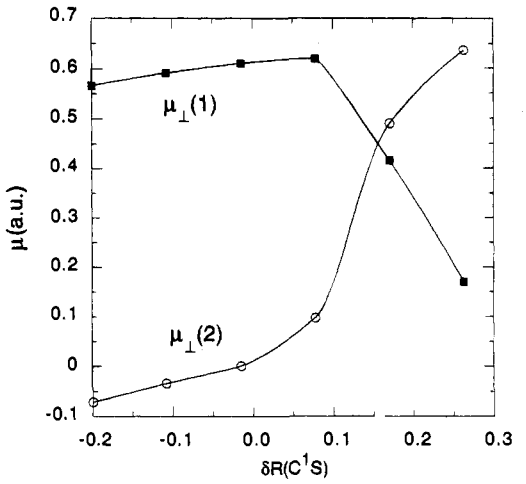

Figure 3. Transition moments $\mu_\perp(j)$, $j = 1$, solid square and $j = 2$, open circle, as a function of $\delta R(C^1S)$ remaining geometrical parameters fixed at the predicted $\tilde{X}^1A_1$ equilibrium structure indicated in Table 1.

Figure 3 reports the interstate electronic transition moments, $\mu_\perp(j) \equiv \langle\Psi(1^1A')|\mu_z|\Psi(j^1A'')\rangle$, $j = 1, 2$, corresponding to the geometries in Figure 2. Note that $\mu_\perp(2) \sim 0$ at $\delta R(C^1S) = 0$ (actually $\mu_\perp(2) = 0.001$ due to small deviations of the reference structure from precise C_{2v} symmetry) identifying the $2^1A''$ state as the valence-like 1^1A_2 state noted in the Introduction. Thus $\mu_\perp(2)$ is a valence–valence transition moment in this region. This result also demonstrates that symmetry breaking does not occur for either the ground or the excited state to any significant extent with the current SA-MCSCF/SOCI description. This is an important consideration in this work which seeks to investigate deviations from C_{2v} geometries. The $1^1A''$ state, for which $\mu_\perp(1) \neq 0$, is identified from an analysis of the wave function as the Rydberg-like 1^1B_2 state at $\delta R(C^1S) = 0$ so that $\mu_\perp(1)$ is a valence-Rydberg transition moment.

From Figure 2 an avoided crossing of the $1,2^1A''$ states is evident for $\delta R(C^1S) \sim 0.15-0.2$ au, that is for distinctly non C_{2v} geometries. From Figure 3 it is seen that at this avoided crossing the valence–valence transition moment $\mu_\perp(2)$ increases, borrowing intensity from the valence–Rydberg transition moment $\mu_\perp(1)$. Thus for dimethyl sulfide in which the C^1SC^2 asymmetric stretch is excited photoexcitation will produce state density on *both* the $1^1A''$ and $2^1A''$ potential energy surfaces. However only the $1^1A''$ potential energy surface correlates with ground state products.

To assess the potential impact of conical intersections on the dissociation of the $2^1A''$ state eq 2.1 was used to locate conical intersections with $R(C^1S) = 3.33$, 3.43, 3.53, and $3.63a_0$, that is $\delta R(C^1S) = -0.16$, -0.06, 0.04, 0.14 and the remaining geometrical parameters *unconstrained*. The results are reported in Table 1, which gives $E(1^1A'')$, $\Delta E \equiv E(2^1A'') - E(1^1A'')$, $R(C^2S)$, $\angle C^1SC^2$, $R(C^iH^j)$, $(i = 1, j = 1,2)$ and $(i = 2, j = 4, 5)$, and $\angle SC^iH^j$, $(i,j) = (1,1)$ and $(2,4)$. The organization of the internal coordinates in this table reflects the intuitive notion that the conical intersection is controlled by the three C^1SC^2 internal coordinates with the CH_3 groups relaxing in response to the C^1SC^2 rearrangement. This interpretation is considered further below. The evaluation of $\mathbf{Q}^{IJ}(\mathbf{R},\xi,\lambda)$ is quite costly for the MCSCF/CI wave functions used in this work. It was expedient therefore to use $\mathbf{Q}^{IJ}(\mathbf{R},\xi,\lambda) = \mathbf{1}$ when solving eq 2.1.[6] As a consequence the iterative solution of eq 2.1 was halted when the magnitude of the right hand side of eq 2.1a was less than 0.5×10^{-2}, which tests showed was sufficient to recover the perponderance of the geometric relaxation effects. The remainder of the right hand side of eq 2.1 is however quite well converged and note in particular that in each case in Table 1 degeneracy, as measured by ΔE, is achieved to <0.7 cm^{-1}—see eq 2.3c and associated discussion. This level for degeneracy is routine with the present algorithm.[10] The conical intersection points are also indicated in Figure 2. For each fixed value of $\delta R(C^1S)$ the conical intersection point is seen to be lower in energy than the otherwise undistorted molecule and accessible with 190–210 nm (47 600–52 600 cm^{-1}) photons. Thus this portion of the surface of conical intersection provides an energetically accessible path for the $2^1A''$ state to dissociate to ground state fragments.

At the conical intersection points the $R(C^iH^j)$ are little changed from their ground state values $r_e(C^iH^j) \sim 2.05$ au. The principal difference between the ground state structure and the conical intersection points is the increase in $R(C^2S)$ from $r_e(CS) \sim 3.49a_0$ to $R(C^2S) \sim 3.7$ a_0 on the surface of conical intersection. The internuclear angles show additional variations. $\angle C^1SC^2$ increases from 105.5° at the equilibrium geometry of the X^1A_1 state to approximately 112° on the surface of conical intersection. However as seen from Table 1 the $\angle SC^iH^j$ also change significantly from their X^1A' equilibrium values, $\angle SC^1H^1 = 104.2°$ and $\angle SC^1H^2 = 112.7°$. Note also that while $\angle C^1SC^2$ changes little along the section of the surface of conical intersection presented in Table 1 $\angle SC^1H^2$ exhibits much larger changes. Thus the intuitive notion that changes in the CH_3 moiety are subordinate to changes in the CSC moiety appears to be an oversimplification.

It is interesting to compare the conical intersections for CH_3SCH_3 reported here with the previous treatments of methyl mercaptan and dihydrogen sulfide. As noted in the Introduction in methyl mercaptan a surface of conical intersection also exists for the $1,2^1A''$ states. However on that surface of conical intersection R(SH), the analog of $R(C^2S)$ here, increases markedly with increases in $R(C^1S)$.[10] This does not occur here suggesting that geometrical changes in C^2H^i, $i = 4$, 6 moiety play a significant role in reaching the surface of conical intersection.

In H_2S the possibility of geometrical changes in the methyl group is absent. However the low-lying excited electronic states are similar in origin to those in $(CH_3)_2S$ and in each molecule C_{2v} crossing seams are possible. This work has focussed on C_s nuclear configurations. However the results at $R(C^1S) = 3.63$ au suggest that the C_s crossings may connect with (symmetry allowed) crossings for C_{2v} nuclear configurations. In H_2S C_{2v} conical intersections are well known.[8] It will be interesting to determine whether C_s conical intersections also exist for this system. Calculations to address this question are currently in progress.

The calculations reported in this section suggest the following model of $(CH_3)_2S$ photodissociation involving the $2^1A''$ state. Excitation of the CSC asymmetric stretch permits population to be generated on (a linear combination of the $1^1A''$ state and) the $2^1A''$ state. The $2^1A''$ state can efficiently dissociate to ground state products by accessing a conical intersection of the $1^1A''$ and $2^1A''$ states. This surface of conical intersections is reached exoergically by stretching the CS bond and distortions of the CH_3 and CSC bond angles. Inclusion of the conical intersections reported in this work in any model of dimethyl sulfide photodissociation appears essential.

IV. Summary and Conclusions

The photodissociation process $CH_3SCH_3(X^1A_1) + h\nu \rightarrow CH_3SCH_3$ $(1^1A_2, 1^1B_2) \rightarrow CH_3(X^2A') + CH_3S(X^2E)$ is considered using configuration interaction wave functions comprised of over 1.2 million configuration state functions. Photons in the range

190−210 nm can produce a superposition of vibrational states on both the $1^1B_2(1^1A'')$ and $1^1A_2(2^1A'')$ potential energy surfaces with states on the later surface produced as the result of vibronic coupling of the 1^1A_2 and 1^1B_2 states through a CSC asymmetric stretch mode. The strength of the intensity borrowing reflects an avoided crossing of these two states in the Franck−Condon region of the X^1A_1 state. The $2^1A''$ state does not dissociate adiabatically to $CH_3(X^2A') + CH_3S(X^2E)$. It can dissociate nonadiabatically to these ground state fragments however, and, in this regard, a surface of conical intersections of the $1,2^1A''$ potential energy surfaces, energetically accessible with 190−210 nm photons must be considered. Points on this surface of conical intersection in the vicinity of the Franck−Condon region of the X^1A_1 state were characterized in this work.

This work has emphasized conical intersections for C_s nuclear configurations and observed simultaneous CSC and CH_3 distortions. It will be interesting to consider the possibility of C_s symmetry conical intersections in H_2S for which CH_3 distortions are not possible. Calculations in this regard are in progress.

Acknowledgment. The calculations reported in this work were performed on D.R.Y.'s IBM RISC 6000 workstations purchased and maintained with funds provided by AFOSR Grant AFOSR 90-0051, NSF Grant CHE 91-03299 and DOE Grant DOE−BES Grant DE-FG02-91ER14189.